

# Could a Neuroscientist Understand a Box of Sand: Lesioning Computational Embeddings within Granular Metamaterials

Piper Welch<sup>1</sup>, Thomas F. Varley<sup>1,2</sup>, Monica Li<sup>3</sup>, Shawn Beaulieu<sup>1</sup>, Corey S. O’Hern<sup>3</sup>,  
Rebecca Kramer-Bottiglio<sup>3</sup>, and Josh Bongard<sup>1</sup>

<sup>1</sup>Department of Computer Science, University of Vermont, Burlington VT, 05404, USA

<sup>2</sup>Vermont Complex Systems Institute, University of Vermont, Burlington VT, 05404, USA

<sup>3</sup>Department of Mechanical Engineering, Yale University, New Haven CT, 06520, USA

piper.welch@uvm.edu

## Abstract

As Moore’s law approaches its terminus, the need for alternative computing paradigms becomes increasingly pressing. A promising alternative exploits mechanical interactions *in materio* to perform computation. One way to achieve this is with computational granular metamaterials (CGMMs), materials that have been optimized to harness mechanical signals such as force, shear, or wave propagation to process information. When materials are designed to perform several computations simultaneously, each at a unique vibrational frequency, the resulting *polycomputational* materials may eventually achieve functional densities superior to traditional computing substrates. However, the relationship between material structure and computational ability is not yet understood. To address this gap, we adopt lesioning methods from neuroscience to probe the structure-function relationship within CGMMs. By systematically disabling grains in optimized configurations, we identify critical components and reveal how specific grains participate in computation. We complement our *in silico* work with a hardware demonstration of a vibrational granular metamaterial, illustrating how future, more complex, and useful CGMMs, designed *in silico*, may be physically realized. These findings offer a new understanding of the computational dynamics of CGMMs, which may suggest ways to further increase their computational density in the future. This may eventually allow them to take their place among the next generation of computing systems in the post-Moore’s Law era.

Code available at: [https://github.com/piperwelch/cgmm\\_lesion](https://github.com/piperwelch/cgmm_lesion)

## Introduction

The invention of the transistor 75 years ago, followed by the integrated circuit, led to continuous miniaturization and cost reduction, famously described by Moore’s Law (Moore et al., 1975). Modern consumer microprocessors now contain over 180 billion transistors (Apple, 2025). However, the pace of transistor miniaturization is predicted to slow, shifting the focus toward alternative computing strategies (Theis and Wong, 2017; Shanbhag et al., 2008). In particular, there has been an emergence of novel computational paradigms that leverage unconventional physical substrates,

architectures, and materials. Such novel computing strategies include quantum computing, neuromorphic computing, DNA computing, and mechanical computing (Horowitz and Grumbling, 2019; van De Burgt et al., 2018; Yasuda et al., 2021).

In this work, we focus on mechanical computing within granular materials. These materials consist of discrete, interacting units that exhibit complex collective dynamics, which can be harnessed to propagate, process, and transform mechanical signals (Jaeger et al., 1996). Computational systems using granular materials, known as computational granular metamaterials (CGMMs), were first introduced by Li et al. in 2014. CGMMs function as Boolean logic gates using mechanical signals. The bit abstraction of these systems can be a variety of mechanical properties, such as vibration or static forces. A marked benefit of CGMMs over other computing paradigms is their ability to support multiple logic gates operating within the same substrate simultaneously. For example, a single CGMM could support two logic gates that both use vibrational oscillation as the bit abstraction, with one operating at frequency  $\omega_1$  and one operating at frequency  $\omega_2$ . This behavior, known as *polycomputation*, offers computational density for which no upper bound has been identified (Parsa et al., 2023). Supplementary Video 1 shows the behavior of a polycomputational material that computes AND at 20 Hz and XOR at 15 Hz.

While computational granular metamaterials offer advantages over the silicon paradigm, they also present unique challenges—chief among them is the unintuitive relationship between their form and function. To produce materials that execute desired logic gates, machine learning has been used to determine how a material’s structure should be configured. Optimization acts on grain properties, such as mass, size, or stiffness, such that a material’s behavior complies with the desired Boolean gate (Parsa et al., 2022a,b, 2023; Beaulieu et al., 2024; Welch et al., 2025a,b). Although optimized CGMMs can implement logical operations, the underlying physical mechanisms by which specific morphological configurations give rise to function remain poorly understood. In effect, CGMMs currently operate as black-box

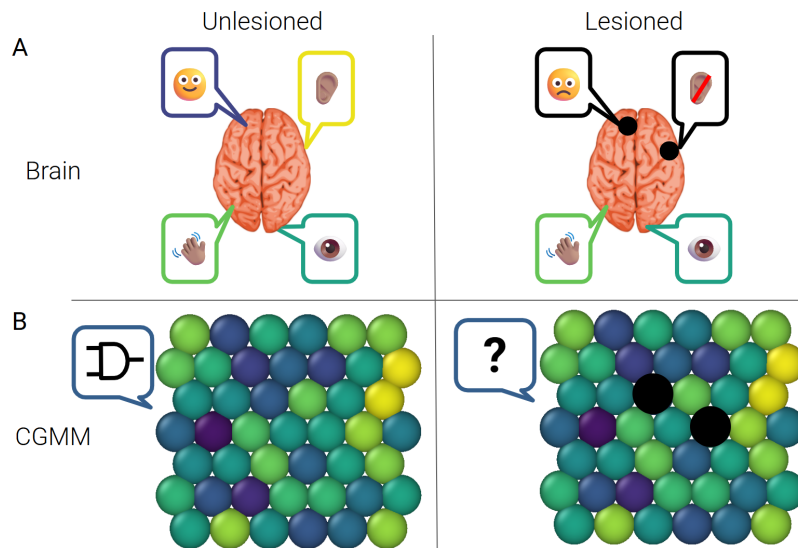


Figure 1: **Overview.** **A)** The top row shows a comparison between an unlesioned brain (left) with intact functions (emotion, hearing, vision, motor control) and a lesioned brain (right) where certain functions are impaired due to targeted damage (indicated by black spots). **B)** The bottom row shows the corresponding CGMM representations: a wild-type configuration (left) optimized to perform Boolean AND, and a lesioned configuration (right) with immobilized grains (black circles), resulting in uncertain function outputs. CGMMs are visualized using OVITO (Stukowski, 2009).

systems. For example, it is unclear whether they rely on a distributed contribution from many grains or operate via a sparse subset of computationally active grains embedded within an otherwise passive lattice. Furthermore, it remains an open question whether different Boolean functions are realized through distinct structural components.

To investigate the internal behavior of black-box systems, researchers in other fields, particularly neuroscience, have employed lesion studies (Vaidya et al., 2019; Adolphs, 2016). These studies involve systematically disabling or removing specific components of a system and observing the resulting changes in behavior. In doing so, they provide insights into the functional roles of individual parts within complex systems (Mullally et al., 2012; Foerde et al., 2013; Shamay-Tsoory et al., 2009; Müller and Knight, 2006).

Motivated by this approach and by Jonas and Kording (2017), we perform a lesion study on CGMMs to investigate the underlying principles governing their behavior. Figure 1 illustrates an overview of our approach. We first employed an evolutionary algorithm to optimize CGMMs to function as either 1) the Boolean logic gate AND, 2) the Boolean logic gate XOR, or 3) the Boolean logic gates AND and XOR simultaneously. We then lesioned optimized designs and analyzed the resulting changes in gate function to better understand the relationship between structure and function in CGMMs. In addition to our *in silico* work, we also provide and perform lesions on a hardware demonstration of vibrational granular metamaterials.

## Methods

### Material Details

In this work, a granular material consists of 45 3D grains arranged in a triangular lattice (Fig. 1B). Each material is within a bounding box featuring fixed boundaries along the  $x$  and  $y$  directions. Both normal and tangential grain interactions adhere to a Hookean contact model. A Hookean model of contact also governs grain interactions with the system boundaries. All grains have the same diameter,  $D=10$  cm, selected arbitrarily.

### Evolving CGMMs

We ran three optimization experiments. In the first two, *monocomputational* materials (those designed to perform a single logic function) were evolved to execute either Boolean AND or XOR at 15 Hz. In the third, *polycomputational* materials (those capable of performing multiple logic functions) were evolved to execute AND at 20 Hz and XOR at 15 Hz. For each experiment, we performed 30 replicates. We used the Wilcoxon rank-sum test and Bonferroni corrections for all statistical analyses with multiple pairwise comparisons.

**System Definitions.** Logical inputs are passed into the material as sinusoidal vibrations supplied to two input grains. The logical output is measured as the vibration of the output grain at the driving frequency. The locations of output and input grains are arbitrary and fixed. True, or ‘1’, is passed into the material as a sinusoidal input of amplitude

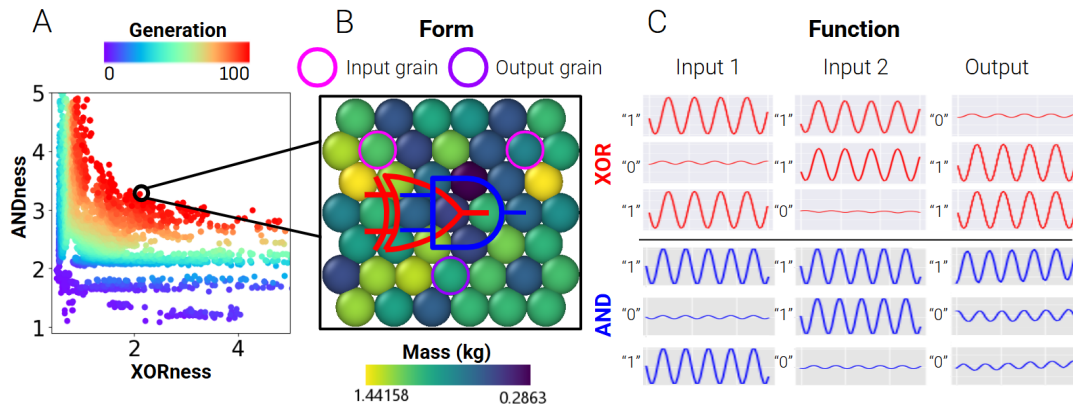


Figure 2: **Form and Function in an Evolved Material.** A) The progression of population fitness over time for one evolutionary run. B) A sample material produced by evolution capable of executing XOR and AND simultaneously. C) The behavior of the optimized CGMM. It successfully executes XOR at the red frequency and AND at the blue frequency.

$A = 0.5$  cm at driving frequency  $\omega_n$  Hz. Conversely, the logical input of False, or ‘0’, is encoded as a sinusoidal input of amplitude  $A = 0$  cm. To quantify output signals, we perform the fast Fourier transformation on the oscillation of the output grain. This converts output signals from the amplitude-time domain to the power-frequency domain. This step is essential for being able to separate logical outputs for different gates in polycomputational materials, as it enables signal disambiguation based on frequency when outputs overlap in space and time.

**Simulation.** We used the open-source software LAMMPS (Large-scale Atomic/Molecular Massively Parallel Simulator) (Thompson et al., 2022) to model our granular materials. We used a time step of 0.001 s and ran our simulations for 2000 steps. All reported units are expressed in SI units.

**Optimization.** To design materials that behave as logic gates, we coupled our physics simulator with a  $(\lambda + \mu)$  evolutionary algorithm, where  $\lambda = 100$  and  $\mu = 200$ .

**Initialization.** The genome of each material is a 45-length array of floats, where each float represents the mass of one grain within the material. Each value in a material’s genome was randomly initialized from a uniform distribution  $\in [0.5 \text{ kg}, 1.3 \text{ kg}]$ . At generation 0, we created 200 materials with randomly generated genomes.

**Evaluation.** After creation, each material had its fitness evaluated. A material has one fitness per gate that is embedded in it. Specifically, monocomputational materials received one fitness from their performance of XOR or AND at 15 Hz, while polycomputational materials received two fitnesses based on their performance of XOR at 15 Hz and AND at 20 Hz. To assess fitness, we evaluated each gate’s

behavior under the ‘01’, ‘10’, and ‘11’ input cases. The ‘00’ input case was omitted as it is arbitrary. We used continuous fitness functions that quantify “GATeness” to enable evolution to follow a gradient. The metric we used to quantify the logical AND behavior of a gate operating at frequency  $\omega_n$ , or “ANDness” is:

$$\text{ANDness} = \frac{\hat{f}_{\omega_n}^{11'}}{(\hat{f}_{\omega_n}^{10'} + \hat{f}_{\omega_n}^{01'})/2} \quad (1)$$

while the metric we used to quantify logical XOR behavior of a gate operating at frequency  $\omega_n$ , or “XORness” is:

$$\text{XORness} = \frac{(\hat{f}_{\omega_n}^{01'} + \hat{f}_{\omega_n}^{10'})/2}{\hat{f}_{\omega_n}^{11'}} \quad (2)$$

We define  $\hat{f}_{\omega_n}^{ij}$  as the power at the driving frequency of the Fourier transform when logical input  $ij$  is supplied to the material. Both of these functions was designed to amplify output signals that should correspond to an output of logical ‘1’ and suppress those that should correspond to an output of logical ‘0’.

**Selection.** After all materials were simulated and their behavior assessed, the materials with the lowest fitness values were removed from our population. For monocomputational materials, survivor selection was performed using tournament selection. For polycomputational materials, survivors were chosen through pairwise comparisons in which two individuals were randomly selected and one was discarded if it is Pareto-dominated. This process repeats until the population size reaches 100.

**Reproduction.** Each of the materials remaining in the population after selection was allowed to reproduce twice.

We employed a mutation operator that acts on each child with a 10% chance of mutating the mass of a given grain in the child’s genome. The mutation size is randomly chosen on a uniform distribution  $\in \pm 0.0525$  kg. Grains have a minimum mass of 0.262 kg and a maximum mass of 5 kg.

We repeated this process of creating, evaluating, and mutating materials until 100 generations have occurred.

### Lesioning CGMMs

After evolution, we selected the materials with the most similar fitnesses across each of the 30 replicates from both the mono- and polycomputational materials to undergo lesioning. A grain is considered “lesioned” when its  $x,y$  position is fixed at its energy-minimized location, and it is assigned an effectively infinite mass. We implemented lesions by freezing the state of individual grains, rather than removing them entirely, as extraction would compromise the stability of the granular lattice. Hence, lesioning effectively removes a grain’s ability to move or transmit force dynamically while preserving its structural presence. Supplementary Video 2 shows a sample material with two lesioned grains. We applied lesions to each of the 42 grains not designated as input or output grains, as modifying these critical grains would compromise the function of the system. Each material was subjected to 42 one-grain lesions, as well as all  $\binom{42}{2}$  possible two-grain lesions. We defined the impact of a given lesion as:

$$1 - \frac{G'_{iO}}{G_O} \quad (3)$$

where  $G'_{iO}$  represents the GATeness measured at the output grain following the lesion of grain  $i$  and  $G_O$  denotes the wild-type GATeness of the material, measured at the output grain. Here, a value of 1 indicates a complete loss of logical functionality, while a value of 0 signifies no measurable effect on gate performance.

### Results

Evolution successfully produced materials capable of executing the target logical functions across all experiments. Figure 2A shows the progression of population fitness over evolutionary time for one experiment in which materials are optimized to perform both AND and XOR. Figure 2B presents a representative evolved CGMM that successfully performs both functions simultaneously. Figure 2C illustrates the behavior of the evolved material, which computes XOR at the red frequency and AND at the blue frequency. Notably, evolution tends to be divergent in these experiments, producing CGMMs with markedly different structural layouts even when optimized for the same functions. Representative examples of this morphological diversity are shown in Supplementary Figure 1.

Descriptive statistics (Table 1) revealed that all CGMMs, both in mono- and polycomputational materials, are highly

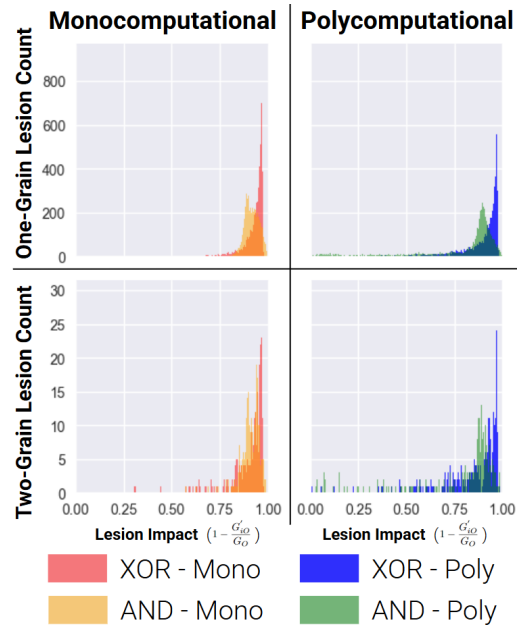


**Figure 3: Distribution of Lesion Impact on Gate Function.** Distribution of lesion impact across different material types for all one- and two-grain lesions. The left column presents polycomputational materials performing both XOR and AND at distinct frequencies (15 Hz and 20 Hz, respectively). The right column shows monocomputational materials executing either XOR or AND at a single frequency (15 Hz).

Gate	Mat. Type	N. lesions	Median $1 - \frac{G'_{iO}}{G_O}$	IQR
XOR	Poly.	1	0.9344	0.1050
AND	Poly.	1	0.8833	0.1462
XOR	Mono.	1	0.9510	0.0486
AND	Mono.	1	0.9138	0.0546
XOR	Poly.	2	0.9116	0.1588
AND	Poly.	2	0.8726	0.2030
XOR	Mono.	2	0.9315	0.0789
AND	Mono.	2	0.9153	0.0574

**Table 1: Descriptive Statistics.** This table presents descriptive statistics summarizing the impact of one and two-grain lesions on logical gate performance across different Boolean gates and material types.

sensitive to lesions. Across all conditions, the median lesion impact ranged from 0.8833 to 0.9510. Figure 3 shows the distribution of one- and two-grain lesion impact on gate function in mono- and polycomputational materials. The impact of lesions on the XOR gates was significantly greater than on the AND gates across both poly and monocomputational materials, for both one- and two-grain lesions

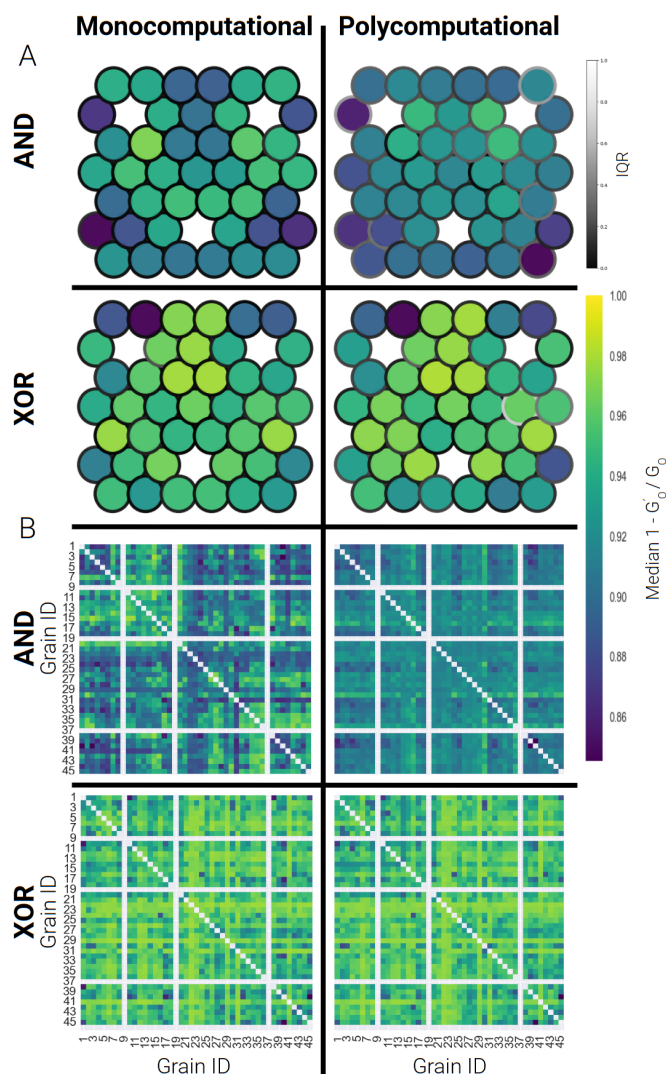


Figure 4: **Median Lesion Impact.** **A)** Heatmaps of single-grain lesion impact on gate function across XOR and AND in mono- and polycomputational materials. Each grain’s face color represents the median impact on gate function caused by lesioning that grain across 30 materials, while the edge color represents the IQR for the lesion. **B)** Matrices showing the median two-grain lesion impact on gate function across XOR and AND in mono- and polycomputational materials. Positions with no data indicate locations of the inputs or output grains.

( $p < 0.05$ ). Two-grain lesions were significantly less damaging than their single lesion counterparts for all comparisons, save for monocomputational materials that compute AND ( $p < 0.05$  for all comparisons), although the effect size is minimal (Table 1). Gates functioning in polycomputational materials exhibited significantly higher variability in their responses to lesions compared to those in monocomputational materials ( $p < 0.05$  for all comparisons).

## Discussion

### Spatial Positioning and Lesion Impact

We proceeded with investigating whether the impact of a lesion depends on the spatial location of the affected grain

or grains within the material’s geometry. Before this study, it was unclear whether certain regions within a CGMM are more functionally critical than others, and, if such regions exist, whether their locations are conserved across different Boolean logic gates. To explore this, we computed per-grain lesion impacts across all lesions. For one-grain lesions, we visualized the median lesion impact as spatial heat maps (Figure 4A). Here, the face color of each grain corresponds to the median impact on gate performance resulting from lesioning that specific grain. The edge color of each grain indicates the IQR of the lesion impacts, reflecting the variability in its effect. Interesting spatial patterns emerge from a close inspection of this figure. For instance, although most

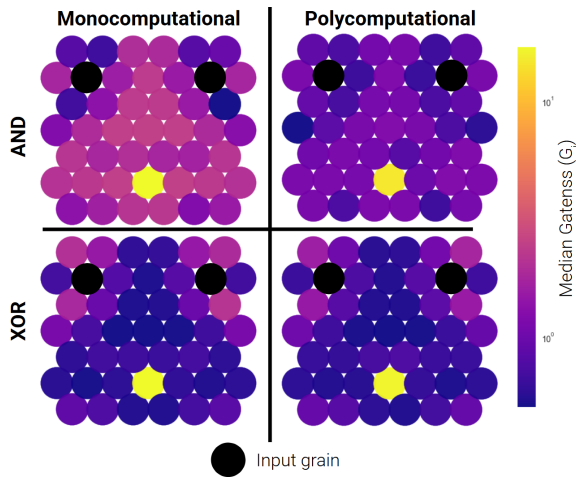


Figure 5: **Median Distribution of Gate Computation.** Heat maps of median grain-level distribution of Boolean logical function for the gates AND (top) and XOR (bottom) gates within mono- and polycomputational materials.

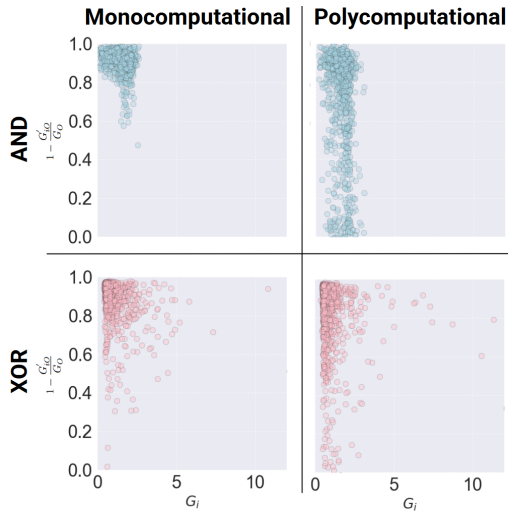


Figure 6: **Lesion Impact and pre-lesion GATeness.** Scatter plots showing pre-lesion GATeness ( $G_i$ ) versus lesion impact ( $1 - \frac{G'_i}{G_O}$ ) for both XOR and AND in mono- and polycomputational materials.

grains exhibit low interquartile ranges, polycomputational materials demonstrate higher variability on a dispersed collection of grains. Furthermore, XOR gates across mono- and polycomputational materials exhibit similar spatial patterns of lesion impact. In both mono- and polycomputational materials, a cluster of grains that almost entirely eliminate gate function is centrally located, between and slightly below the input grains, which suggests a conserved region important for XOR function. Furthermore, lesions on the grains above the inputs have a relatively smaller impact on

gate function. This spatial asymmetry indicates that not all regions contribute equally to computational integrity and that the functional architecture of XORs is slightly more robust to disruptions in certain peripheral zones. In contrast, AND gates show more divergent patterns across material types. In monocomputational materials, AND gates display a linear arrangement of high-impact grains extending from the inputs toward the center of the material, suggesting a structurally defined pathway that is functionally significant. Polycomputational AND gates lack a continuous region of high sensitivity, instead showing a scattered distribution of impactful grains near the inputs, while grains closer to the output appear less critical to function.

Figure 4B shows the impact of each two-grain lesion on logic gate performance. Each cell in a given matrix represents the impact of lesioning a specific pair of grains. The matrix entry at position  $(i, j)$  quantifies the functional loss resulting from simultaneously lesioning grains  $i$  and  $j$ . Supplementary Figure 2 reports the IQR of the functional impact for lesions involving each individual grain. Several notable patterns emerge within these matrices. Specifically, certain lesions that induce a great reduction in gate function when paired with most other grains may exhibit a diminished effect when combined with a particular second lesion. This phenomenon is especially pronounced in the XOR gates of both mono- and polycomputational materials. On the other hand, lesioning certain grains remains highly detrimental regardless of how two lesions are combined. Another noteworthy pattern is that the XOR matrices exhibit more similarity to one another than to the AND matrices, while the AND matrices show greater mutual similarity, indicating that lesion interaction patterns are conserved for different Boolean logic gates.

Interestingly, although the XOR and AND gates in polycomputational materials operate concurrently within the same substrate, given lesions impacted them differently. The co-localization of logic functions in polycomputational materials does not guarantee uniform vulnerability; instead, each gate type appears to rely on distinct substructures or pathways to achieve its behavior. This implies a form of internal functional compartmentalization, where different logical operations are distributed across overlapping but distinct subsets of grains. Such compartmentalization may be advantageous for fault tolerance, allowing one function to remain relatively intact even when another is impaired by the same lesion.

### Gate Embodiment and Lesion Impact

We next investigated the relationship between the degree of GATeness present at a given grain in the wild-type material and the impact of lesioning it. We were motivated by the hypothesis that grains with a high degree of GATeness may act as critical nodes. They could be key contributors whose structural or functional integrity is essential for the

material to correctly execute a given logic gate. If this is true, lesioning such grains should disproportionately impair gate performance. We define  $G_i$  as the GATeness (Eqn. 1,2) as measured at grain  $i$ . Figure 5 shows heat maps of the median grainwise  $G_i$  spatially distributed in XOR and AND across each grain for mono- and polycomputational materials. Across both material types, we observe similar spatial patterns of GATeness for XORs. Namely, there are relatively high  $G_i$  grains localized above the input grains, and lower  $G_i$  grains elsewhere. In contrast, the monocomputational AND gate shows a more diffuse distribution of  $G_i$ , while in the polycomputational AND,  $G_i$  is slightly lower and more evenly reduced across all grains. Figure 6 presents scatter plots of  $G_i$  and  $1 - \frac{G'_i}{G_i}$  for XOR and AND gates across mono- and polycomputational materials. Unintuitively, across all experiments, we observe no clear relationship between  $G_i$  and the relative degradation in gate function following a lesion. This result indicates that grains with a high embodiment of a Boolean function do not consistently serve as critical points whose disruption leads to large functional impairment.

### Lesions and Information Integration

In keeping with the analogy with neuroscience, we next studied how lesions changed functional patterns of correlations between grains in monocomputational materials (analogous to functional connectivity networks in brains (Sporns, 2010)). Briefly, we computed covariance matrices from the z-scored displacement time series for each grain. We then computed the total correlation (Varley et al., 2023). For zero-mean and unit variance data, the total correlation of a covariance matrix can be estimated as:

$$TC(\mathbf{X}) = \frac{-\ln|\Sigma_{\mathbf{X}}|}{2} \quad (4)$$

where  $|\Sigma_{\mathbf{X}}|$  is the determinant of the covariance matrix of multivariate time series  $\mathbf{X}$ . TC quantifies the overall deviation from independence: a greater value suggests greater global integration. We can then quantify the effect of a lesion following the immobilization of a grain:

$$\Delta^{-i}TC(\mathbf{X}) = TC(\mathbf{X}) - TC(\mathbf{X}^{-i}) \quad (5)$$

Where  $\mathbf{X}^{-i}$  is the new time series generated after a single-grain lesion. A positive value suggests a decrease in integration following a lesion, while a negative value would suggest an increase in integration post-lesion. We found that, when a set of 25 CGMMs evolved to compute the logical AND received the ‘01’ or ‘10’ input cases, on average,  $\approx 68\%$  of the materials had  $\Delta^{-i}TC(\mathbf{X}) > 0$  nat, the remaining 32% were negative. This suggests that, when the CGMMs are receiving a single input, the effects of lesions are functionally heterogeneous. In contrast, when materials received the ‘11’ input case, the effects of lesioning

became functionally homogeneous: all but two of the CGMMs showed  $\Delta^{-i}TC(\mathbf{X}) > 0$ , indicating that the effects of lesions change depending on the structure of the inputs. The pattern was the same when considering a population of monocomputational XOR gates.

Finally, we considered the extent to which the CGMMs could be said to “integrate” functional information in ways that are irreducible to pairwise interactions (i.e. to what extent the CGMMs are capable of displaying “emergent” coordination). To test this, we computed a variant of the Whole-Minus-Sum integrated information (Balduzzi and Tononi, 2008):

$$\Phi_{ij}^{WMS}(\mathbf{X}) = \Delta^{ij}TC(\mathbf{X}) - [\Delta^iTC(\mathbf{X}) + \Delta^jTC(\mathbf{X})] \quad (6)$$

If  $\Phi_{ij}^{WMS}() > 0$ , then the change in the total correlation when both  $X_i$  and  $X_j$  are lesioned is greater than the change we would expect based on the two lesions considered alone: there is some non-trivial interaction between the grains that is only observable when both lesions are present simultaneously. Said differently, the system is “vulnerable” to multiple failure, as the influence of both compound. In contrast, if  $\Phi_{ij}^{WMS} < 0$ , then the change produced by the two lesions is of lower magnitude than the sum of the “parts”, suggesting robustness of multiple failures.

In a single CGMM evolved to compute a logical AND gate, we found a mixture of positive and negative values of  $\Phi_{ij}^{WMS}$  (see Supplementary Fig. 3). These results suggest that evolved CGMMs combine features of both redundancy (robustness to multiple lesions) and information integration (which brings vulnerability to multiple lesions), which is consistent with prior work suggesting that functional complexity balances trade-offs between information integration and redundancy (Varley and Bongard, 2024).

### Hardware Implementation

To ground our computational findings, we constructed a physical prototype of a granular logic gate. Specifically, we hand-designed a vibrational granular substrate that functions as a physical analog of the identity operation. We then explored the impact of lesions on the behavior of this physical granular substrate.

**Grain & Bounding Box Construction.** We fabricated ten grains out of 6.35 mm (1/4 inch) thick cast acrylic. Each grain is 25.4 mm (1 inch) in diameter. We created an outer bounding box that was similarly laser cut from cast acrylic. We dimensioned the bounding box for ten grains in a hexagonal packing. We accounted for the thickness of the laser beam such that the grains are rigidly constrained in the box. We fixed the bounding box to the workspace table using two clamps, ensuring rigid constraint during the experiment.

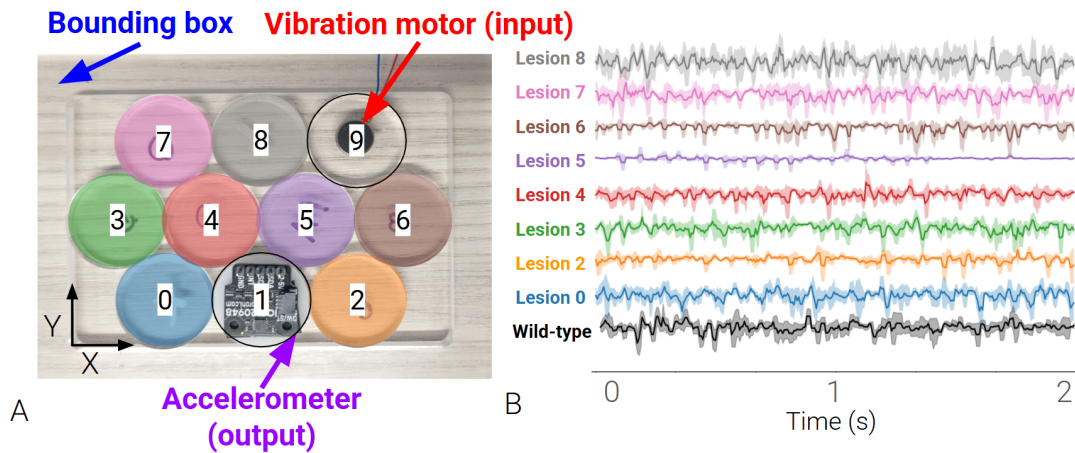


Figure 7: **Hardware Implementation.** **A)** Configuration of our granular lattice implementation in hardware. **B)** The y-direction acceleration of the output grain resulting from various lesions. Data are plotted as an EEG waveform display to facilitate viewing multiple signals within the same range.

**Vibration Motor & Accelerometer.** We supply input vibrations to a grain using a coin motor with an eccentric mass. The motor is 10 mm in diameter and 3 mm thick. The motor is connected to a 5V power supply and oscillates at 300 Hz. We fixed the motor to the center of Grain 9 using an adhesive backing. We fabricated an overhang to constrain out-of-plane motion, thereby preventing the vibrating grain from dislodging or vibrating beyond the boundaries of the containment box. We measured vibrational output signals in the y-direction by mounting an accelerometer (ICM20948 9DoF Motion Sensor, Breakout PIM448) on Grain 1. We sampled acceleration at 166 Hz.

**Lesion Experiments.** Lesions were realized in hardware by applying localized pressure to a given grain with a compliant surface. Contact both dampened the vibrations and restricted a lesioned grain’s movement. We recorded acceleration for two seconds for each lesion in the packing. We lesioned each grain in the packing five times.

**Findings.** From Fig. 7, which shows the mean and standard deviation of y-direction acceleration across five trials, we observe that lesioning different grains has varying effects on the vibrational amplitude of the output grain. Lesioning Grain 5 results in a significantly reduced amplitude of acceleration of the output grain ( $p < 0.05$ ), while lesioning other grains, with the exception of Grain 8, shows no significant difference from the wild type. This result is intuitive because the shortest mechanical pathway between the input and output passes through Grain 5. Counterintuitively, lesioning Grain 8 leads to a marginally significant increase in the amplitude of acceleration of the output grain ( $p < 0.07$ ). We hypothesize that this occurs because energy is redirected through Grains 5 and 6 when Grain 8

is immobilized, resulting in amplified vibration at the output.

This vibrational hardware platform provides a potential testbed for transferring optimized grain configurations from simulation to physical implementation (sim2real). While the current system is unary with a single source of input vibration, it could be extended to binary logic by incorporating a second motor. Then, we could run optimization over grain properties such as mass, stiffness, and size. However, such a study is beyond the scope of this work.

## Conclusions & Future Work

In this work, we sought to investigate the structure–function relationship in CGMMs by adapting lesion studies from neuroscience. By selectively perturbing components of these systems, we aimed to understand how localized disruptions influence global computational behavior. Our findings show that CGMMs are highly sensitive to lesions, with near-universal degradation in logic gate execution following introduced disruptions. Moreover, we observe that different instantiations of the same Boolean gate exhibit similar patterns of functional impact from lesions.

Several avenues of future research are warranted. First, we aim to pursue the sim2real transfer of evolved logic gates. Understanding how evolved designs retain or lose functionality with the physical constraints of real-world materials is critical for improving the simulator, and ultimately for enabling the deployment of these logic gates in future computing systems. We also plan to extend the application of lesions to include a broader spectrum of perturbations, such as those that arise through material fatigue, structural degradation, or heterogeneous failure modes, thereby better approximating the environmental and operational challenges such systems may encounter.

## Acknowledgments

This material is based upon work supported by the National Science Foundation Graduate Research Fellowship Program under Grant No. 2235204. Any opinions, findings, and conclusions or recommendations expressed in this material are those of the author(s) and do not necessarily reflect the views of the National Science Foundation. We would also like to acknowledge financial support from the National Science Foundation under the DMREF program (award number: 2118810)

## References

- Adolphs, R. (2016). Human lesion studies in the 21st century. *Neuron*, 90(6):1151–1153.
- Apple (2025). Apple reveals M3 Ultra, taking Apple silicon to a new extreme.
- Balduzzi, D. and Tononi, G. (2008). Integrated information in discrete dynamical systems: motivation and theoretical framework. *PLoS computational biology*, 4(6):e1000091.
- Beaulieu, S., Welch, P., Parsa, A., O’Hern, C., Kramer-Bottiglio, R., and Bongard, J. (2024). Refractive Computation: parallelizing logic gates across driving frequencies in a mechanical polycomputer. In *ALIFE 2024: Proceedings of the 2024 Artificial Life Conference*. MIT Press.
- Foerde, K., Race, E., Verfaellie, M., and Shohamy, D. (2013). A role for the medial temporal lobe in feedback-driven learning: evidence from amnesia. *Journal of Neuroscience*, 33(13):5698–5704.
- Horowitz, M. and Grumbling, E. (2019). Quantum computing: progress and prospects.
- Jaeger, H. M., Nagel, S. R., and Behringer, R. P. (1996). The physics of granular materials. *Physics today*, 49(4):32–38.
- Jonas, E. and Kording, K. P. (2017). Could a neuroscientist understand a microprocessor? *PLoS computational biology*, 13(1):e1005268.
- Li, F., Anzel, P., Yang, J., Kevrekidis, P. G., and Daraio, C. (2014). Granular acoustic switches and logic elements. *Nature communications*, 5(1):5311.
- Moore, G. E. et al. (1975). Progress in digital integrated electronics. volume 21, pages 11–13. Washington, DC.
- Mullally, S. L., Intraub, H., and Maguire, E. A. (2012). Attenuated boundary extension produces a paradoxical memory advantage in amnesic patients. *Current Biology*, 22(4):261–268.
- Müller, N. G. and Knight, R. T. (2006). The functional neuroanatomy of working memory: contributions of human brain lesion studies. *Neuroscience*, 139(1):51–58.
- Parsa, A., Wang, D., O’Hern, C. S., Shattuck, M. D., Kramer-Bottiglio, R., and Bongard, J. (2022a). Evolving programmable computational metamaterials. In *Proceedings of the Genetic and Evolutionary Computation Conference*, pages 122–129.
- Parsa, A., Wang, D., O’Hern, C. S., Shattuck, M. D., Kramer-Bottiglio, R., and Bongard, J. (2022b). Evolution of Acoustic Logic Gates in Granular Metamaterials. In *International Conference on the Applications of Evolutionary Computation (Part of EvoStar)*, pages 93–109. Springer.
- Parsa, A., Witthaus, S., Pashine, N., O’Hern, C., Kramer-Bottiglio, R., and Bongard, J. (2023). Universal Mechanical Poly-computation in Granular Matter. In *Proceedings of the Genetic and Evolutionary Computation Conference*, pages 193–201.
- Shamay-Tsoory, S. G., Aharon-Peretz, J., and Perry, D. (2009). Two systems for empathy: a double dissociation between emotional and cognitive empathy in inferior frontal gyrus versus ventromedial prefrontal lesions. *Brain*, 132(3):617–627.
- Shanbhag, N. R., Mitra, S., de Veciana, G., Orshansky, M., Marculescu, R., Roychowdhury, J., Jones, D., and Rabaey, J. M. (2008). The search for alternative computational paradigms. *IEEE Design & Test of Computers*, 25(4):334–343.
- Sporns, O. (2010). *Networks of the Brain*. MIT Press.
- Stukowski, A. (2009). Visualization and analysis of atomistic simulation data with ovito—the open visualization tool. *Modelling and simulation in materials science and engineering*, 18(1):015012.
- Theis, T. N. and Wong, H.-S. P. (2017). The End of Moore’s Law: A New Beginning for Information Technology. *Computing in science & engineering*, 19(2):41–50.
- Thompson, A. P., Aktulga, H. M., Berger, R., Bolintineanu, D. S., Brown, W. M., Crozier, P. S., in ’t Veld, P. J., Kohlmeyer, A., Moore, S. G., Nguyen, T. D., Shan, R., Stevens, M. J., Tranchida, J., Trott, C., and Plimpton, S. J. (2022). LAMMPS - a flexible simulation tool for particle-based materials modeling at the atomic, meso, and continuum scales. *Comp. Phys. Comm.*, 271:108171.
- Vaidya, A. R., Pujara, M. S., Petrides, M., Murray, E. A., and Fellows, L. K. (2019). Lesion studies in contemporary neuroscience. *Trends in cognitive sciences*, 23(8):653–671.
- van De Burgt, Y., Melianas, A., Keene, S. T., Malliaras, G., and Salleo, A. (2018). Organic electronics for neuromorphic computing. *Nature Electronics*, 1(7):386–397.
- Varley, T. F. and Bongard, J. (2024). Evolving higher-order synergies reveals a trade-off between stability and information-integration capacity in complex systems. *Chaos: An Interdisciplinary Journal of Nonlinear Science*, 34(6):063127.
- Varley, T. F., Pope, M., Faskowitz, J., and Sporns, O. (2023). Multivariate information theory uncovers synergistic subsystems of the human cerebral cortex. *Communications Biology*, 6(1):1–12. Number: 1 Publisher: Nature Publishing Group.
- Welch, P., Li, M., Beaulieu, S., Xia, A., Wang, D., Goyal, M., Parsa, A., O’Hern, C., Kramer-Bottiglio, R., and Bongard, J. (2025a). Greater AI Design Control Aids Evolution of Computational Materials. In *International Conference on the Applications of Evolutionary Computation (Part of EvoStar)*. Springer.

Welch, P., Parsa, A., Beaulieu, S., , O'Hern, C. S., Kramer-Bottiglio, R., and Bongard, J. (2025b). Evolution of logically independent polycomputational granular metamaterials. In *International Conference on the Applications of Evolutionary Computation (Part of EvoStar)*. Springer.

Yasuda, H., Buskohl, P. R., Gillman, A., Murphey, T. D., Stepney, S., Vaia, R. A., and Raney, J. R. (2021). Mechanical computing. *Nature*, 598(7879):39–48.